

1 **Stress granule-inducing eukaryotic translation initiation factor 4A inhibitors block influenza A**
2 **virus replication**
3

4 Patrick D. Slaine¹, Mariel Kleer¹, Nathan Smith², Denys A. Khaperskyy^{1,*} and Craig McCormick^{1,*}

5
6 ¹Department of Microbiology and Immunology, Dalhousie University, 5850 College Street, Halifax NS,
7 Canada B3H 4R2

8 ²Department of Community Health and Epidemiology, Dalhousie University, 5790 University Avenue,
9 Halifax NS, Canada B3H 1V7
10

11

12

13

14

15

16

17

18

19

20

21

22 *Co-corresponding authors: Denys A. Khaperskyy¹, E-mail: d.khaperskyy@dal.ca ; Craig
23 McCormick¹, E-mail: craig.mccormick@dal.ca

24

25 **Mailing address:** Department of Microbiology and Immunology, Dalhousie University, 5850 College
26 Street, Halifax NS, Canada B3H 4R2. Tel: 1(902) 494-4519

27

28 **Running Title:** eIF4A inhibitors block influenza A virus replication

29

30 **Keywords:** influenza A virus/pateamine A/silvestrol/eIF4A/helicase/stress granule

31

31 **ABSTRACT**

32 Eukaryotic translation initiation factor 4A (eIF4A) is a helicase that facilitates assembly of the translation
33 preinitiation complex by unwinding structured mRNA 5' untranslated regions. Patamine A (PatA) and
34 silvestrol are natural products that disrupt eIF4A function and arrest translation, thereby triggering the
35 formation of cytoplasmic aggregates of stalled preinitiation complexes known as stress granules (SGs).
36 Here we examined the effects of eIF4A inhibition by PatA and silvestrol on influenza A virus (IAV)
37 protein synthesis and replication in cell culture. Treatment of infected cells with either PatA or silvestrol
38 at early times post-infection results in SG formation, arrest of viral protein synthesis and failure to
39 replicate the viral genome. PatA, which irreversibly binds to eIF4A, sustained long-term blockade of IAV
40 replication following drug withdrawal, and inhibited IAV replication at concentrations that had minimal
41 cytotoxicity. By contrast, the antiviral effects of silvestrol were fully reversible; drug withdrawal caused
42 rapid SG dissolution and resumption of viral protein synthesis. IAV inhibition by silvestrol was invariably
43 associated with cytotoxicity. PatA blocked replication of genetically divergent IAV strains, suggesting
44 common dependence on host eIF4A activity. This study demonstrates the feasibility of targeting core host
45 protein synthesis machinery to prevent viral replication.

46 **IMPORTANCE**

47 Influenza A virus (IAV) relies on cellular protein synthesis to decode viral messenger RNAs. Pateamine
48 A and silvestrol are natural products that inactivate an essential protein synthesis protein known as eIF4A.
49 Here we show that IAV is sensitive to these eIF4A inhibitor drugs. Treatment of infected cells with
50 pateamine A or silvestrol prevented synthesis of viral proteins, viral genome replication and release of
51 infectious virions. The irreversible eIF4A inhibitor pateamine A sustained long-term blockade of viral
52 replication, whereas viral protein synthesis quickly resumed after silvestrol was removed from infected
53 cells. Prolonged incubation of either infected or uninfected cells with these drugs induced the
54 programmed cell death cascade called apoptosis. Our findings suggest that core components of the host
55 protein synthesis machinery are viable targets for antiviral drug discovery. The most promising drug
56 candidates should selectively block protein synthesis in infected cells without perturbing bystander
57 uninfected cells.

58 INTRODUCTION

59 Influenza A viruses (IAV) are enveloped viruses with segmented, negative-sense single-stranded RNA
60 genomes (vRNAs) that primarily infect epithelial cells in a diverse range of hosts. The viruses bind to
61 cell surface sialic acids and are internalized by endocytosis. The virus gains access to the cytoplasm
62 following the fusion of viral and endosome membranes. Viral genome segments are then imported into
63 the cell nucleus, where viral mRNA synthesis is initiated by the viral RNA-dependent RNA polymerase
64 (RdRp) complex, which cleaves nascent host RNA polymerase II (pol II)-transcribed RNAs at sites 10-14
65 nucleotides downstream of 5' 7-methyl-guanosine (m7G) caps (1). These short capped RNAs are used to
66 prime viral mRNA synthesis. Template-directed viral mRNA synthesis is terminated by reiterative
67 decoding of short uridine-rich sequences, which generates 3'-poly-adenylate (polyA) tails. Thus, by
68 coupling a trimeric RdRp complex to each incoming genome segment, the virus ensures faithful
69 generation of mRNAs with 5'-caps and polyA tails that largely resemble host mRNAs.

70 Efficient translation of IAV mRNAs depends on virus-mediated suppression of host gene expression, a
71 process known as host shutoff. Host shutoff gives viral mRNAs priority access to the host protein
72 synthesis machinery. IAV host shutoff mechanisms identified to date encompass different stages of host
73 mRNA biogenesis. The viral PA-X endoribonuclease selectively targets host pol II transcripts while
74 sparing viral mRNAs, as well as pol I and pol III transcripts (2). In addition, the viral nonstructural-1
75 (NS1) protein binds and inhibits cleavage and polyadenylation specificity factor 30 kDa subunit
76 (CPSF30), an essential component of the host 3' end processing machinery for cellular pre-mRNAs that
77 is dispensable for viral mRNA processing (3). NS1 also enhances the association between newly-
78 synthesized viral mRNAs and cellular NXF1/Tap mRNA export factors (4), while simultaneously
79 inhibiting nucleoporin 98 (Nup98)-mediated export of host mRNAs (5). In addition to host shutoff, there
80 is evidence that efficient translation of viral mRNAs depends on short, conserved cis-acting sequences in

81 viral 5' untranslated regions (UTRs), downstream of the host-derived leader sequences (6). It is not
82 known precisely how these 5'-UTR sequences assist translation, but recent work has shown that when
83 bound to viral mRNAs, the NS1 protein plays an important role in ribosome recruitment (7). By contrast,
84 recent studies employing RNA-sequencing, ribosomal foot-printing and single-molecule fluorescence in-
85 situ hybridization have suggested that host shutoff is mainly achieved by reduction in cellular mRNA
86 levels, and that IAV mRNAs are not preferentially translated (8). It is clear that viral proteins enable
87 efficient translation of IAV mRNAs, but the precise composition of translation pre-initiation complexes
88 assembled on these mRNAs, and the contribution of diverse host translation initiation factors remains
89 incompletely characterized.

90 Dependence on host protein synthesis machinery makes viral mRNAs sensitive to various stress-induced
91 translation repression mechanisms. A particularly critical checkpoint in translation initiation is the
92 assembly of the ternary complex, comprised of eIF2, GTP and tRNAi^{met}, which allows for incorporation
93 of the tRNAi^{met} into the 40S ribosomal subunit. This step is negatively regulated by serine
94 phosphorylation of eIF2 by one of four kinases: heme-regulated translation inhibitor (HRI), general
95 control non-derepressible-2 (GCN2), protein kinase R (PKR) and PKR-like endoplasmic reticulum kinase
96 (PERK) (9). eIF2 phosphorylation causes accumulation of stalled 48S preinitiation complexes and
97 associated mRNA transcripts, which are bound by aggregation-prone RNA-binding proteins, including
98 Ras-GAP SH3 domain-binding protein (G3BP), T-cell intracellular antigen-1 (TIA-1), and TIA-1 related
99 protein (TIAR). These complexes nucleate cytoplasmic stress granules (SGs), sites where stalled mRNP
100 complexes are triaged, until stress is resolved and protein synthesis can resume.

101 IAV mRNAs are efficiently translated throughout infection and SGs never form (10). IAV prevents
102 translation arrest, at least in part, through the action of NS1, a double-stranded RNA (dsRNA)-binding
103 protein that prevents PKR-mediated eIF2 α phosphorylation. We have shown previously that IAV encodes

104 two additional proteins, PA-X and NP, that block SG formation in an eIF2 α -independent manner (11).
105 Precise details of NP and PA-X mechanism of action remain obscure, but SG-inhibition by PA-X is
106 tightly linked to its host shutoff function, as it requires endonuclease activity. This mechanism is
107 reminiscent of the herpes simplex virus-type 2 (HSV-2) virion host shutoff (vhs) protein, which also
108 requires endonuclease activity to prevent SG formation (12). Taken together, these findings suggest that
109 IAV dedicates a significant portion of its small genome to encode proteins with SG-antagonizing activity.
110 SG suppression is maximal at late times post-infection, coinciding with the accumulation of NS1, NP and
111 PA-X proteins. We have shown previously that at early times post-infection, treatment of infected cells
112 with sodium arsenite, which causes HRI activation and eIF2 α phosphorylation, triggered SG formation
113 and stalled viral replication (11). Thus, like host mRNAs, at early times post-infection, IAV mRNAs are
114 exquisitely sensitive to eIF2 α phosphorylation and ternary complex depletion. We have also shown that
115 IAV mRNAs are sensitive to pateamine A (PatA) (11), a natural product that selectively inhibits the
116 DEAD-box RNA helicase eIF4A which assembles with eIF4E and eIF4G, to form the eIF4F complex
117 (13, 14). By disrupting eIF4A, PatA prevents scanning by the 43S pre-initiation complex, causing arrest
118 of translation initiation, and inducing SG formation (15). Specifically, treatment with PatA caused SG
119 formation at early times post-infection and diminished accumulation of viral proteins.

120 In addition to PatA, eIF4A can be inhibited by a variety of natural compounds currently being
121 investigated for anti-cancer properties, including hippuristanol (16), 15-deoxy-delta 12,14-
122 prostaglandin J2 (15d-PGJ2) (17), silvestrol (18) and synthetic derivatives. Accumulating evidence
123 indicates that many viruses are highly dependent on eIF4A activity for protein synthesis. For example,
124 PatA has been shown to limit human cytomegalovirus infection (19), whereas silvestrol has been shown
125 to inhibit Ebola virus replication (20).

126 In this study, we methodically documented the antiviral properties of PatA and silvestrol in three
127 workhorse models of IAV infection; A549 human lung adenocarcinoma cells, Madin-Darby canine
128 kidney (MDCK) cells, and African green monkey kidney epithelial cells (Vero). In all cases, dosages of
129 PatA and silvestrol sufficient to elicit SGs concurrently blocked viral protein accumulation and genome
130 replication. PatA, known to bind irreversibly to eIF4A, could sustain long-term arrest of viral protein
131 synthesis following drug withdrawal, whereas the effects of silvestrol were reversible. Finally, PatA could
132 inhibit genetically-divergent strains, suggesting common dependence on eIF4A.

133

134

135 **MATERIALS AND METHODS**

136 **Reagents and cells**

137 Unless specifically indicated, all chemicals were purchased from Sigma. Pateamine A was a kind gift
138 from Dr. Jerry Pelletier (McGill University, Montreal, QC, Canada), silvestrol was obtained from
139 MedChem Express (Princeton, NJ); 1 mM stocks of silvestrol and pateamine A were prepared in DMSO
140 and stored at -80°C. A549, Vero and Madin-Darby Canine Kidney (MDCK) cells were maintained in
141 Dulbecco's modified Eagle's medium (DMEM; HyClone) supplemented with 10% fetal bovine serum
142 (FBS, Life Technologies) and 100 U/ml penicillin + 100 µg/ml streptomycin + 20 µM L-glutamine
143 (Pen/Strep/Gln; Wisent) at 37°C in 5% CO₂ atmosphere. All cell lines were purchased from the American
144 Type Culture Collection (ATCC).

145

146 **Viruses, infections and treatments**

147 Influenza virus strains used in this study include A/PuertoRico/8/34/(H1N1) virus (PR8) and
148 A/Udorn/1972(H3N2) virus (Udorn). Unless specified otherwise, infections were conducted at a
149 multiplicity of infection (MOI) of 1. After inoculation, cells were washed with 1x PBS and incubated
150 with infection medium containing 0.5% bovine serum albumin (BSA) in DMEM and incubated at 37°C in
151 5% CO₂ atmosphere. IAV virions were enumerated by plaque assay using 1.2% Avicel RC 591 (FMC
152 Corporation) overlay on confluent MDCK cells as described in (21). Where indicated, mock and virus-
153 infected cells were treated with 0.156-40 nM pateamine A or 2.5-640 nM silvestrol.

154

155 **Cell viability measurement**

156 Cells were seeded 24 h before drug treatment at a density of 10,000 cells/well in 96-well plates. Drugs
157 were serially-diluted in media to the indicated concentrations and added to cells. After 24-h treatment,

158 AlamarBlue assay (Thermo Scientific) was conducted according to manufacturer's protocol using Tecan
159 Infinite M200 PRO microplate reader (excitation = 560 nm, emission = 590 nm). Values were normalized
160 to vehicle control.

161

162 **Immunostaining**

163 For immunofluorescence microscopy cells grown on glass coverslips were fixed and stained as described
164 previously (11) using mouse monoclonal antibody to G3BP (clone 23, BD Transduction Labs), goat
165 polyclonal antibody to influenza virus (ab20841, Abcam), and rabbit monoclonal antibody to TIAR
166 (clone D32D3, Cell Signaling) at manufacturer-recommended dilutions. Donkey Alexa Fluor-conjugated
167 secondary antibodies (Molecular Probes) were used at 1:1000 dilution in combination with 5 ng/ml
168 Hoechst dye. Images were captured using Zeiss Axioplan II microscope or Zeiss LSM 510 laser scanning
169 microscope. For western blot analysis, whole cell lysates were resolved on TGX Stain-Free Precast Gels
170 (BioRad) and analyzed using goat polyclonal antibody to influenza virus described above (recognizes
171 HA1, NP, and M1 proteins), mouse monoclonal antibodies to influenza NS1 (clone 13D8, reference (22)),
172 puromycin (MABE343, Millipore Sigma), and rabbit antibodies to phospho-Ser-51-eIF2 α (D9G8, Cell
173 Signaling), PARP (9542S, Cell Signaling), and β -actin (13E5, HRP-conjugated, Cell Signaling).

174

175 **Real time quantitative PCR**

176 Total RNA was isolated using the RNeasy Plus Mini kit (Qiagen) according to manufacturer's protocol.
177 Viral genomic and messenger RNAs were reverse-transcribed as described in (2) using Maxima H Minus
178 Reverse Transcriptase (Thermo Scientific) in separate reactions containing the gene-specific primer for
179 18S rRNA (5'-AGG GCC TCA CTA AAC CAT CC-3') and either the influenza A virus-specific
180 universal primer Uni12 (5'-AGC AAA AGC AGG-3', for vRNA) or the oligo(dT)₁₈ primer (for mRNA).

181 Quantitative PCR analysis was performed using GoTaq PCR master mix (Promega). Relative initial
182 template quantities were determined using the Ct method. Primer sequences and the PCR thermal profile
183 setup are available upon request.

184

185

186 **RESULTS**

187 **Pateamine A and silvestrol induce stress granules and inhibit viral protein accumulation in dose-**
188 **dependent manner.**

189 We previously demonstrated that IAV was sensitive to pharmacologic induction of translation arrest and
190 SG formation in the early stages of infection (11). To gain a fuller understanding of how eIF4A-targeting
191 drugs can trigger SG formation and disrupt viral replication, IAV-infected A549, Vero and MDCK cells
192 were treated at 1 hpi with increasing doses of PatA and silvestrol. In all three cell lines, PatA triggered SG
193 formation and inhibited IAV protein accumulation at concentrations above 2.5 nM (Fig. 1A-D). By
194 contrast, SG formation was triggered in response to 40 nM silvestrol in infected A549 cells, and 160 nM
195 silvestrol in infected MDCK cells. Remarkably, Vero cells were highly resistant to translation arrest and
196 SG induction by silvestrol. For both PatA and silvestrol, SG induction tightly correlated with inhibition of
197 viral protein synthesis across all three cell lines.

198

199 **Pateamine A is more potent than silvestrol at inhibiting viral replication in cultured cells**

200 Previously, we demonstrated that 10 nM PatA blocked IAV replication in A549 cells through sustained
201 total protein synthesis arrest and SG formation (11). To further test the effects of PatA and silvestrol on
202 infectious virus release in the three most common cell culture models of IAV infection, we treated A549,
203 Vero and MDCK cells with increasing concentrations of these drugs at 1 h post-infection with the PR8
204 strain of IAV. At 24 hpi, culture supernatants were harvested and the infectious virus titers were
205 determined using plaque assays in MDCK cells (Fig. 2A, B). In agreement with results presented in Fig.
206 1, 5 nM PatA was sufficient to reduce virus replication 10-fold in all three cell lines while silvestrol had
207 minimal effect on virus replication in Vero cells. In MDCK cells, silvestrol was much less effective at
208 inhibiting infectious virus release; 16-times higher drug concentration was required to match the inhibition

209 of infectious virion release observed in A549 cells. Overall, these results reveal tight correlation between
210 viral protein accumulation and the infectious virus production in these cell lines, and the unexpected
211 remarkable resistance of Vero cells to silvestrol. Next, we tested the effects of PatA and silvestrol on cell
212 viability after 24 h treatment using the AlamarBlue assay (Fig. 2C, D). Both drugs exhibited notable
213 cytotoxicity at the concentrations required for maximal inhibition of virus replication. However, the
214 cytotoxic effects varied significantly between the cell lines tested. 5 nM PatA had little effect on A549
215 cells, but it caused a sharp decrease in viability of MDCK cells. By contrast, among the three cell types,
216 A549 cells were most sensitive to silvestrol. Taken altogether, these results suggest that PatA is more
217 effective than silvestrol at inhibiting virus replication at sub-cytotoxic concentrations and exhibits a
218 narrow therapeutic index in A549 cells.

219

220 **Silvestrol withdrawal causes SG dissolution and resumption of viral protein accumulation.** PatA and
221 silvestrol have distinct molecular structures and mechanisms of eIF4A disruption. Both molecules induce
222 eIF4A dimerization and force an engagement with RNA, thereby depleting eIF4A from eIF4F complexes
223 and inhibiting cap-dependent translation (14, 23). However, PatA has been shown to be an irreversible
224 translation inhibitor (13), whereas silvestrol-dependent translation inhibition occurs reversibly (16). These
225 distinct properties provided a unique opportunity to investigate whether IAV can ‘recover’ from SG
226 formation following withdrawal of the SG-inducing drug. To address this directly, IAV-infected A549
227 cells were incubated with 30 nM PatA or 300 nM silvestrol starting from 1 hpi. At 4 hpi, drug was
228 washed off of some infected cells, and SG formation and viral protein accumulation were analyzed using
229 immunofluorescence microscopy at 12 hpi (Fig. 3A). Consistent with our previous observations (11),
230 after withdrawal of PatA, SGs persisted for the remainder of the time-course, and viral proteins did not
231 accumulate beyond the levels observed at 1 hpi. However, silvestrol withdrawal at 4 hpi led to SG

232 disassembly and robust IAV protein accumulation; thus, ‘wash-off’ (WO) reversed the effects of
233 silvestrol. To confirm that SG dissolution due to silvestrol withdrawal coincides with the resumption of
234 protein synthesis, we treated A549 cells with silvestrol or PatA and labelled newly synthesized proteins
235 with a 10 min pulse of puromycin at various times post-treatment (24). The newly-synthesized peptides
236 were visualized by western blot (Fig. 3B). Both silvestrol and PatA caused strong inhibition of protein
237 synthesis at 1 h post-treatment, which was sustained throughout the 24 h treatment time-course. Silvestrol
238 withdrawal at 3 h allowed for a complete restoration of protein synthesis at later times (Fig. 3B, lanes 7
239 and 12). By contrast, protein synthesis was never restored following PatA wash-off (Fig. 3B, lanes 8 and
240 13). Together, these findings demonstrate that IAV is able to recover from transient drug-induced
241 translation arrest and resume the viral replication cycle when eIF4A inhibition is relieved.

242

243 **Prolonged eIF4A inhibition triggers apoptosis**

244 SG formation promotes cell survival in response to a variety of environmental stresses (9). However, the
245 SG-inducing eIF4A inhibitors silvestrol and PatA have been shown to promote apoptosis of cancer cells
246 (23, 25–27). Moreover, apoptosis is a well-described feature of late-stage IAV infection, required for
247 efficient virion production (28–31). To determine whether eIF4A disruption affects the fate of IAV-
248 infected cells in our system, both infected and uninfected A549 cells were treated with 300 nM silvestrol
249 or 30 nM PatA, and apoptosis was measured by immunoblotting for PARP cleavage products. Following
250 16 h incubation with drugs, PARP cleavage species accumulated in both mock-infected and IAV-infected
251 cells alike, indicating that sustained eIF4A disruption overcomes any pro-survival effects of SG
252 formation, resulting in apoptosis (Fig. 4A, lanes 5-8). Interestingly, the sustained translation arrest by
253 silvestrol not only diminished viral protein accumulation, but also prevented the RdRp from switching
254 tasks between viral mRNA synthesis and genome replication (Fig. 4B). This finding is consistent with our

255 previous observations for PatA (11), suggesting that both drugs affect the viral replication cycle in the
256 same way. This dysregulated RdRp activity and an inability to produce the viral PKR antagonist NS1 due
257 to translation arrest, enables detection of viral pathogen-associated molecular patterns (PAMPs), resulting
258 in eIF2 α phosphorylation (Fig. 4, lanes 5-6).

259

260 **Effects of silvestrol and pateamine A on IAV replication are not strain-specific**

261 We have determined that the lab-adapted H1N1 PR8 strain used in this study, which is the preferred
262 backbone for vaccine production worldwide, is sensitive to eIF4A inhibition. To determine whether a
263 genetically-divergent IAV strain could be similarly affected by eIF4A inhibiting drugs, A549 cells were
264 infected with the H3N2 Udorn strain. Infected cells were treated with 300 nM silvestrol at 4 hpi, and the
265 viral RNA and protein accumulation was determined over a 12 h time-course. Consistent with our
266 previous findings using the PR8 strain, silvestrol treatment affected RdRp switching from viral mRNA
267 synthesis to viral genome replication tasks (Fig. 5A, B) due to failure to accumulate viral proteins (Fig.
268 5C). Our findings to date indicate that PatA is better than silvestrol at inhibiting PR8 replication at sub-
269 cytotoxic doses. For this reason, we investigated the effects of PatA on release of Udorn from A549 cells.
270 We observed a similar magnitude of inhibition of Udorn virion production in cells treated with low
271 nanomolar doses of PatA.

272 **DISCUSSION**

273 IAV mRNAs generally resemble host mRNAs, which enables efficient translation by host cell machinery.
274 However, these features also make them susceptible to stress-induced arrest of protein synthesis. Host
275 translation initiation requires eIF4A, a helicase that unwinds mRNA secondary structure to permit ternary
276 complex scanning for translation initiation codons. Here, we showed that IAV translation is sensitive to
277 the eIF4A inhibitors PatA and silvestrol. These drugs limited viral protein accumulation and elicited the
278 formation of SGs. Because progression through the viral replication cycle depends on accumulation of
279 key viral proteins, these eIF4A inhibitors prevent the viral polymerase complex from switching from viral
280 mRNA synthesis to viral genome replication. Both molecules could block replication of genetically-
281 divergent IAV strains, PR8 and Udorn, suggesting a potential universal dependence on eIF4A activity.
282 While the effects of silvestrol were reversible, PatA, known to bind irreversibly to eIF4A, sustained long-
283 term arrest of viral protein synthesis following drug withdrawal.

284
285 Because many oncogenes have structured 5'-UTRs, and depend on eIF4A activity for their synthesis,
286 eIF4A inhibitors like PatA and silvestrol, have been extensively studied for anti-cancer activity. Low
287 doses of PatA have been shown to inhibit proliferation of tumor xenografts without appreciable toxicity in
288 murine models (32). Indeed, PatA was able to inhibit oncogene synthesis at low doses that did not
289 impinge on bulk protein synthesis rates, demonstrating that mRNA structure plays a crucial role in
290 determining susceptibility and dose-dependent effects of eIF4A inhibitors. As in cancer cells, efficient
291 virus replication typically demands sustained high rates of protein synthesis, which may likewise be
292 dependent on eIF4A helicase activity. For example, Ebola virus has been shown to be exquisitely
293 sensitive to eIF4A inhibition by silvestrol (20). Ebola virus mRNAs have highly-structured 5'-UTRs (33–
294 35) and require processive helicase activity of eIF4A. By contrast, IAV mRNA 5'-UTRs are relatively

295 short, and comprised of divergent host-derived mRNA segments fused to conserved viral mRNA
296 segments. The heterogeneous nature of these 5'-UTRs challenges RNA structure prediction algorithms,
297 but the short, conserved regions do not display significant secondary structure that would necessitate high
298 eIF4A activity. Consistent with this, IAV mRNA translation is inhibited by relatively high doses of
299 silvestrol and PatA that would be predicted to deplete eIF4A from translation preinitiation complexes.
300 Our results and previous studies indicate that eIF4A helicase activity is required for translation initiation
301 on IAV mRNAs, but it appears that processive unwinding of long, structured 5'-UTRs is not required.
302 Consistent with this model, IAV infection was shown to deplete the eIF4A processivity factor eIF4B (36).
303 The virus replicates efficiently in eIF4B-depleted cells, and likely benefits from diminished synthesis of
304 eIF4B-dependent interferon-stimulated genes like IFITM3. Viral mRNP complexes likely lack eIF4B, but
305 remain only partially characterized. They have properties that distinguish them from host mRNPs. For
306 example, there is some evidence that eIF4E1 is also dispensable for viral mRNA translation (37).
307 Moreover, IAV NS1 is known to stimulate viral mRNA translation, which may be linked to its ability to
308 bind to viral mRNP complexes through interactions with eIF4G1 and PABP (38). A better understanding
309 of the precise composition of viral mRNP complexes will likely inform our understanding of the role
310 played by eIF4A and other core translation factors. Beyond these considerations of mRNP composition,
311 dependence on eIF4A helicase activity might also be influenced by host shutoff, which is expected to
312 markedly influence the availability of host translation factors.

313

314 We previously established that SGs do not form at any point during IAV infection (10), and that three
315 viral proteins can inhibit SG formation (11). We also demonstrated that an early window of opportunity
316 exists, before sufficient quantities of SG antagonizing viral proteins accumulate, when the virus is
317 exquisitely sensitive to stress-induced translation arrest. Here, we further elucidated the mechanism of

318 action of SG-inducing eIF4A inhibitors PatA and silvestrol. To date, most of our observations of SGs
319 formed in IAV-infected cells indicate that these granules have canonical composition and properties.
320 Throughout our studies, SG formation in infected cells reliably indicated disruption of viral protein
321 accumulation and viral replication (10, 11). In this study, we observed that, upon withdrawal of silvestrol,
322 SGs rapidly dissolved when viral protein synthesis resumed. At the same time, ongoing translation arrest
323 triggered by PatA resulted in persistence of SGs throughout the observation period. It has been recently
324 demonstrated that PKR is recruited to SGs by direct interaction with G3BP, and that this recruitment
325 results in PKR activation (39, 40). We observe eIF2 α phosphorylation in infected cells after prolonged
326 SG induction by PatA or silvestrol. It will be interesting to determine whether this phosphorylation is
327 dependent on PKR activation.

328

329 Our results show the magnitude of the threat that host-targeted translation inhibitors pose for viral
330 replication. Nevertheless, the eIF4A inhibitors studied here have some undesirable properties that may be
331 difficult to surmount. We observed that eIF4A inhibition resulted in cytotoxic effects that largely tracked
332 with viral inhibition in all cell lines examined. The human (A549), dog (MDCK) and green monkey
333 (Vero) cell lines studied here displayed markedly different sensitivities to silvestrol treatment, which
334 cannot be explained by structural differences in eIF4A because all three isoforms of eIF4A (eIF4A-I, -II,
335 and -III) are highly conserved between these species. Interestingly, while silvestrol has been shown to
336 bind to eIF4A-I and eIF4A-II, PatA has been shown to bind to all three isoforms, including eIF4A-III (32,
337 41–43). While eIF4A-I and eIF4A-II function in the cytoplasm, eIF4A-III is localized to the nucleus and
338 thus has no role in translation initiation. Instead, it is a member of the exon junction complex deposited
339 on mRNA post-splicing, where it has been shown to participate in nonsense mediated decay (44).
340 Moreover, eIF4AIII was previously shown to interact with the IAV polymerase complex (45). The

341 functional significance of this interaction is unknown, and the contribution of eIF4A-III inhibition by
342 PatA to its antiviral effects remain to be determined.

343
344 There is an outstanding need for new antivirals for influenza. Past history has shown that direct-acting
345 antivirals are often rendered ineffective by rapid viral evolution. For this reason, host-targeted antivirals
346 are an attractive alternative approach that should limit the emergence of drug-resistant variants. RNA
347 silencing screens have shown that influenza virus replication depends on thousands of host genes, some of
348 which may be potential candidates for therapeutic intervention. Our data indicates that inhibition of viral
349 protein synthesis potently disrupts the viral replication cycle, and drugs that can block viral protein
350 synthesis may serve as attractive candidates for host-directed antivirals. Despite their antiviral activity
351 against IAV at high doses, PatA and silvestrol appear to lack specificity for viral translation complexes,
352 and impede bulk translation in infected and uninfected cells alike. This distinguishes IAV from other
353 viruses (e.g. Ebola, HCMV) and from cancer models, which were shown to be exquisitely sensitive to
354 much lower doses of eIF4A inhibitor. For these reasons, an effective host-targeted antiviral translation
355 inhibitor for influenza will ideally be specific for infected cells, while sparing uninfected cells.
356 Alternatively, a detailed characterization of IAV mRNP complexes could highlight unique features that
357 could be exploited by future antivirals.

358 **ACKNOWLEDGEMENTS**

359 We thank members of the McCormick lab for critical reading of the manuscript. We thank Drs. Kevin
360 Coombs (University of Manitoba, Winnipeg, MB, Canada), Yoshihiro Kawaoka (University of
361 Wisconsin-Madison, Madison, WI, USA), Jerry Pelletier (McGill University, Montreal, QC, Canada), and
362 Richard Webby (St. Jude Children's Hospital, Memphis, TN, USA) for reagents. We thank Dr. Stephen
363 Whitefield at the Dalhousie University Faculty of Medicine Cellular & Molecular Digital Imaging Core
364 Facility for microscopy support. This work was supported by CIHR Operating Grants MOP-136817 and
365 PJT 148727, and NSERC Discovery Grant RGPIN/341940-2012.

366 **REFERENCES**

- 367 1. Plotch, S. J., M. Bouloy, I. Ulmanen, and R. M. Krug. 1981. A unique cap(m7GpppXm)-dependent
368 influenza virion endonuclease cleaves capped RNAs to generate the primers that initiate viral RNA
369 transcription. *Cell* 23: 847-858.
- 370 2. Khapersky, D. A., S. Schmaling, J. Larkins-Ford, C. McCormick, and M. M. Gaglia. 2016.
371 Selective Degradation of Host RNA Polymerase II Transcripts by Influenza A Virus PA-X Host
372 Shutoff Protein. *PLoS Pathog* 12: e1005427.
- 373 3. Nemeroff, M. E., S. M. Barabino, Y. Li, W. Keller, and R. M. Krug. 1998. Influenza virus NS1
374 protein interacts with the cellular 30 kDa subunit of CPSF and inhibits 3' end formation of cellular
375 pre-mRNAs. *Mol Cell* 1: 991-1000.
- 376 4. Pereira, C. F., E. K. C. Read, H. M. Wise, M. J. Amorim, and P. Digard. 2017. Influenza A Virus
377 NS1 Protein Promotes Efficient Nuclear Export of Unspliced Viral M1 mRNA. *J Virol* 91:
- 378 5. Satterly, N., P. L. Tsai, J. van Deursen, D. R. Nussenzveig, Y. Wang, P. A. Faria, A. Levay, D. E.
379 Levy, and B. M. Fontoura. 2007. Influenza virus targets the mRNA export machinery and the nuclear
380 pore complex. *Proc Natl Acad Sci U S A* 104: 1853-1858.
- 381 6. Garfinkel, M. S., and M. G. Katze. 1993. Translational control by influenza virus. Selective
382 translation is mediated by sequences within the viral mRNA 5'-untranslated region. *J Biol Chem* 268:
383 22223-22226.
- 384 7. Panthu, B., O. Terrier, C. Carron, A. Traversier, A. Corbin, L. Balvay, B. Lina, M. Rosa-Calatrava,
385 and T. Ohlmann. 2017. The NS1 Protein from Influenza Virus Stimulates Translation Initiation by
386 Enhancing Ribosome Recruitment to mRNAs. *J Mol Biol*

- 387 8. Bercovich-Kinori, A., J. Tai, I. A. Gelbart, A. Shitrit, S. Ben-Moshe, Y. Drori, S. Itzkovitz, M.
388 Mandelboim, and N. Stern-Ginossar. 2016. A systematic view on influenza induced host shutoff.
389 *Elife* 5:
- 390 9. Yamasaki, S., and P. Anderson. 2008. Reprogramming mRNA translation during stress. *Curr Opin*
391 *Cell Biol* 20: 222-226.
- 392 10. Khaperskyy, D. A., T. F. Hatchette, and C. McCormick. 2012. Influenza A virus inhibits cytoplasmic
393 stress granule formation. *FASEB J* 26: 1629-1639.
- 394 11. Khaperskyy, D. A., M. M. Emara, B. P. Johnston, P. Anderson, T. F. Hatchette, and C. McCormick.
395 2014. Influenza A virus host shutoff disables antiviral stress-induced translation arrest. *PLoS Pathog*
396 10: e1004217.
- 397 12. Finnen, R. L., T. J. Hay, B. Dauber, J. R. Smiley, and B. W. Banfield. 2014. The HSV-2 Virion-
398 associated Ribonuclease, vhs, Interferes with Stress Granule Formation. *J Virol*
- 399 13. Low, W. K., Y. Dang, T. Schneider-Poetsch, Z. Shi, N. S. Choi, W. C. Merrick, D. Romo, and J. O.
400 Liu. 2005. Inhibition of eukaryotic translation initiation by the marine natural product pateamine A.
401 *Mol Cell* 20: 709-722.
- 402 14. Bordeleau, M. E., R. Cencic, L. Lindqvist, M. Oberer, P. Northcote, G. Wagner, and J. Pelletier.
403 2006. RNA-mediated sequestration of the RNA helicase eIF4A by Pateamine A inhibits translation
404 initiation. *Chem Biol* 13: 1287-1295.
- 405 15. Dang, Y., N. Kedersha, W. K. Low, D. Romo, M. Gorospe, R. Kaufman, P. Anderson, and J. O. Liu.
406 2006. Eukaryotic initiation factor 2alpha-independent pathway of stress granule induction by the
407 natural product pateamine A. *J Biol Chem* 281: 32870-32878.
- 408 16. Lindqvist, L., and J. Pelletier. 2009. Inhibitors of translation initiation as cancer therapeutics. *Future*
409 *Med Chem* 1: 1709-1722.

- 410 17. Kim, W. J., J. H. Kim, and S. K. Jang. 2007. Anti-inflammatory lipid mediator 15d-PGJ2 inhibits
411 translation through inactivation of eIF4A. *EMBO J* 26: 5020-5032.
- 412 18. Bordeleau, M. E., F. Robert, B. Gerard, L. Lindqvist, S. M. Chen, H. G. Wendel, B. Brem, H.
413 Greger, S. W. Lowe, J. A. Porco, and J. Pelletier. 2008. Therapeutic suppression of translation
414 initiation modulates chemosensitivity in a mouse lymphoma model. *J Clin Invest* 118: 2651-2660.
- 415 19. Ziehr, B., E. Lenarcic, C. Cecil, and N. J. Moorman. 2016. The eIF4AIII RNA helicase is a critical
416 determinant of human cytomegalovirus replication. *Virology* 489: 194-201.
- 417 20. Biedenkopf, N., K. Lange-Grünweller, F. W. Schulte, A. Weißer, C. Müller, D. Becker, S. Becker, R.
418 K. Hartmann, and A. Grünweller. 2017. The natural compound silvestrol is a potent inhibitor of
419 Ebola virus replication. *Antiviral Res* 137: 76-81.
- 420 21. Matrosovich, M., T. Matrosovich, W. Garten, and H. D. Klenk. 2006. New low-viscosity overlay
421 medium for viral plaque assays. *Virology* 3: 63.
- 422 22. Rahim, M. N., M. Selman, P. J. Sauder, N. E. Forbes, W. Stecho, W. Xu, M. Lebar, E. G. Brown,
423 and K. M. Coombs. 2013. Generation and characterization of a new panel of broadly reactive anti-
424 NS1 mAbs for detection of influenza A virus. *J Gen Virol* 94: 593-605.
- 425 23. Cencic, R., M. Carrier, G. Galicia-Vázquez, M. E. Bordeleau, R. Sukarieh, A. Bourdeau, B. Brem, J.
426 G. Teodoro, H. Greger, M. L. Tremblay, J. A. Porco, and J. Pelletier. 2009. Antitumor activity and
427 mechanism of action of the cyclopenta[b]benzofuran, silvestrol. *PLoS One* 4: e5223.
- 428 24. Goodman, C. A., P. Pierre, and T. A. Hornberger. 2012. Imaging of protein synthesis with
429 puromycin. *Proc Natl Acad Sci U S A* 109: E989; author reply E990.
- 430 25. Hood, K. A., L. M. West, P. T. Northcote, M. V. Berridge, and J. H. Miller. 2001. Induction of
431 apoptosis by the marine sponge (Mycale) metabolites, mycalamide A and pateamine. *Apoptosis* 6:
432 207-219.

- 433 26. Kim, S., B. Y. Hwang, B. N. Su, H. Chai, Q. Mi, A. D. Kinghorn, R. Wild, and S. M. Swanson.
434 2007. Silvestrol, a potential anticancer rocaglate derivative from *Aglaia foveolata*, induces apoptosis
435 in LNCaP cells through the mitochondrial/apoptosome pathway without activation of executioner
436 caspase-3 or -7. *Anticancer Res* 27: 2175-2183.
- 437 27. Mi, Q., S. Kim, B. Y. Hwang, B. N. Su, H. Chai, Z. H. Arbieva, A. D. Kinghorn, and S. M. Swanson.
438 2006. Silvestrol regulates G2/M checkpoint genes independent of p53 activity. *Anticancer Res* 26:
439 3349-3356.
- 440 28. Wurzer, W. J., O. Planz, C. Ehrhardt, M. Giner, T. Silberzahn, S. Pleschka, and S. Ludwig. 2003.
441 Caspase 3 activation is essential for efficient influenza virus propagation. *EMBO J* 22: 2717-2728.
- 442 29. Wurzer, W. J., C. Ehrhardt, S. Pleschka, F. Berberich-Siebelt, T. Wolff, H. Walczak, O. Planz, and S.
443 Ludwig. 2004. NF-kappaB-dependent induction of tumor necrosis factor-related apoptosis-inducing
444 ligand (TRAIL) and Fas/FasL is crucial for efficient influenza virus propagation. *J Biol Chem* 279:
445 30931-30937.
- 446 30. McLean, J. E., E. Datan, D. Matassov, and Z. F. Zakeri. 2009. Lack of Bax prevents influenza A
447 virus-induced apoptosis and causes diminished viral replication. *J Virol* 83: 8233-8246.
- 448 31. Tran, A. T., J. P. Cortens, Q. Du, J. A. Wilkins, and K. M. Coombs. 2013. Influenza virus induces
449 apoptosis via BAD-mediated mitochondrial dysregulation. *J Virol* 87: 1049-1060.
- 450 32. Kuznetsov, G., Q. Xu, L. Rudolph-Owen, K. Tendyke, J. Liu, M. Towle, N. Zhao, J. Marsh, S.
451 Agoulnik, N. Twine, L. Parent, Z. Chen, J. L. Shie, Y. Jiang, H. Zhang, H. Du, R. Boivin, Y. Wang,
452 D. Romo, and B. A. Littlefield. 2009. Potent in vitro and in vivo anticancer activities of des-methyl,
453 des-amino pateamine A, a synthetic analogue of marine natural product pateamine A. *Mol Cancer*
454 *Ther* 8: 1250-1260.

- 455 33. Mühlberger, E., M. Weik, V. E. Volchkov, H. D. Klenk, and S. Becker. 1999. Comparison of the
456 transcription and replication strategies of marburg virus and Ebola virus by using artificial replication
457 systems. *J Virol* 73: 2333-2342.
- 458 34. Weik, M., J. Modrof, H. D. Klenk, S. Becker, and E. Mühlberger. 2002. Ebola virus VP30-mediated
459 transcription is regulated by RNA secondary structure formation. *J Virol* 76: 8532-8539.
- 460 35. Schlereth, J., A. Grünweller, N. Biedenkopf, S. Becker, and R. K. Hartmann. 2016. RNA binding
461 specificity of Ebola virus transcription factor VP30. *RNA Biol* 13: 783-798.
- 462 36. Wang, S., X. Chi, H. Wei, Y. Chen, Z. Chen, S. Huang, and J. L. Chen. 2014. Influenza A virus-
463 induced degradation of eukaryotic translation initiation factor 4B contributes to viral replication by
464 suppressing IFITM3 protein expression. *J Virol* 88: 8375-8385.
- 465 37. Burgui, I., E. Yángüez, N. Sonenberg, and A. Nieto. 2007. Influenza virus mRNA translation
466 revisited: is the eIF4E cap-binding factor required for viral mRNA translation. *J Virol* 81: 12427-
467 12438.
- 468 38. Burgui, I., T. Aragon, J. Ortin, and A. Nieto. 2003. PABP1 and eIF4GI associate with influenza virus
469 NS1 protein in viral mRNA translation initiation complexes. *J Gen Virol* 84: 3263-3274.
- 470 39. Reineke, L. C., J. D. Dougherty, P. Pierre, and R. E. Lloyd. 2012. Large G3BP-induced granules
471 trigger eIF2alpha phosphorylation. *Mol Biol Cell* 23: 3499-3510.
- 472 40. Reineke, L. C., N. Kedersha, M. A. Langereis, F. J. van Kuppeveld, and R. E. Lloyd. 2015. Stress
473 granules regulate double-stranded RNA-dependent protein kinase activation through a complex
474 containing G3BP1 and Caprin1. *MBio* 6: e02486.
- 475 41. Bordeleau, M. E., J. Matthews, J. M. Wojnar, L. Lindqvist, O. Novac, E. Jankowsky, N. Sonenberg,
476 P. Northcote, P. Teesdale-Spittle, and J. Pelletier. 2005. Stimulation of mammalian translation

- 477 initiation factor eIF4A activity by a small molecule inhibitor of eukaryotic translation. *Proc Natl*
478 *Acad Sci U S A* 102: 10460-10465.
- 479 42. Low, W. K., Y. Dang, S. Bhat, D. Romo, and J. O. Liu. 2007. Substrate-dependent targeting of
480 eukaryotic translation initiation factor 4A by pateamine A: negation of domain-linker regulation of
481 activity. *Chem Biol* 14: 715-727.
- 482 43. Korneeva, N. L. 2007. Translational dysregulation by Pateamine A. *Chem Biol* 14: 5-7.
- 483 44. Palacios, I. M., D. Gatfield, D. St Johnston, and E. Izaurralde. 2004. An eIF4AIII-containing
484 complex required for mRNA localization and nonsense-mediated mRNA decay. *Nature* 427: 753-
485 757.
- 486 45. Watanabe, T., E. Kawakami, J. E. Shoemaker, T. J. Lopes, Y. Matsuoka, Y. Tomita, H. Kozuka-
487 Hata, T. Gorai, T. Kuwahara, E. Takeda, A. Nagata, R. Takano, M. Kiso, M. Yamashita, Y. Sakai-
488 Tagawa, H. Katsura, N. Nonaka, H. Fujii, K. Fujii, Y. Sugita, T. Noda, H. Goto, S. Fukuyama, S.
489 Watanabe, G. Neumann, M. Oyama, H. Kitano, and Y. Kawaoka. 2014. Influenza virus-host
490 interactome screen as a platform for antiviral drug development. *Cell Host Microbe* 16: 795-805.
491

492 **FIGURE LEGENDS**

493 **Figure 1. Concentration-dependent stress granule induction and inhibition of viral protein**

494 **accumulation by pateamine A and silvestrol.** A549, Vero, and MDCK cell lines infected with PR8
495 strain of IAV were treated with the indicated concentrations of pateamine A (PatA) or silvestrol (Sil.) at 1
496 hpi. (A-C) Viral protein accumulation was analysed in whole cell lysates collected at 24 hpi using western
497 blot. (D) Stress granule induction and viral protein accumulation were visualized at 9 hpi by
498 immunofluorescence microscopy using antibody to stress granule marker TIAR (red) and the polyclonal
499 anti-influenza antibody (green). Nuclei were stained with Hoechst dye (blue). Representative images are
500 shown for each cell line and treatment condition.

501

502 **Figure 2. Antiviral and cytotoxic effects of pateamine A and silvestrol vary between cell types.** (A,

503 B) Production of infectious virus progeny (PR8 strain) at 24 hpi was measured using plaque assay. The
504 indicated cell lines were infected with MOI = 0.1 and treated with the increasing concentrations of
505 pateamine A (A) or silvestrol (B) at 1 hpi. (C, D) Cell viability was measured using Alamar Blue assay
506 after 24-h treatment with increasing concentrations of pateamine A (C) or silvestrol (D). Relative
507 fluorescence values are normalized to vehicle control (DMSO). (A-D) Error bars represent standard
508 deviations from 3 independent biological replicates.

509

510 **Figure 3. Translation inhibition by silvestrol is fully reversible.** (A) A549 cells infected with PR8

511 strain of IAV were treated at 1 hpi with 320 nM silvestrol (Sil.) or 20 nM pateamine A (PatA) or left
512 untreated. At 4 hpi, some wells were washed briefly with PBS and received fresh infection media without
513 drugs as shown on the schematic outline of the experiment. At 12 hpi mock and virus-infected cells
514 subjected to continuous incubation with Sil. or PatA or to drug wash off at 4 hpi (WO) were analysed by

515 immunofluorescence staining with the polyclonal anti-influenza antibody (IAV, green) and the antibodies
516 to SG markers TIAR (red) and G3BP (blue). (B) Total translation rates in A549 cells were analyzed using
517 metabolic labelling with puromycin and subsequent western blotting with anti-puromycin antibody. In
518 some cases, after initial 3-h treatments, Sil. or PatA were washed off (WO) prior to puromycin labeling.
519 Total protein was visualized using BioRad Stain-Free reagent.

520

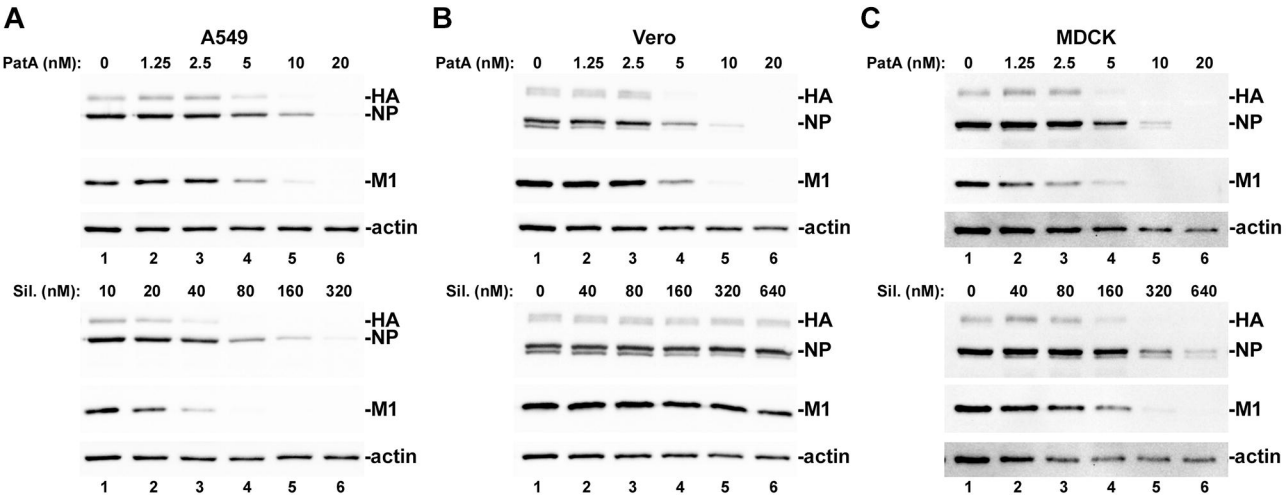
521 **Figure 4. Sustained eIF4A inhibition by silvestrol and pateamine A leads to induction of apoptosis.**

522 (A) Western blotting analysis of A549 cell lysates obtained at the indicated times post-infection with the
523 PR8 strain of IAV and treated with 320 nM silvestrol (Sil.) or 20 nM pateamine A (PatA) at 4 hpi or the
524 equivalent time after mock infection. (B) Total RNA was isolated from cells treated with 320 nM
525 silvestrol at 4 hpi and the relative levels of viral NS1 mRNA and vRNA at the indicated times post-
526 infection were determined using RT-qPCR. Error bars represent standard deviations (n=3). P values were
527 calculated using paired Student's t-test.

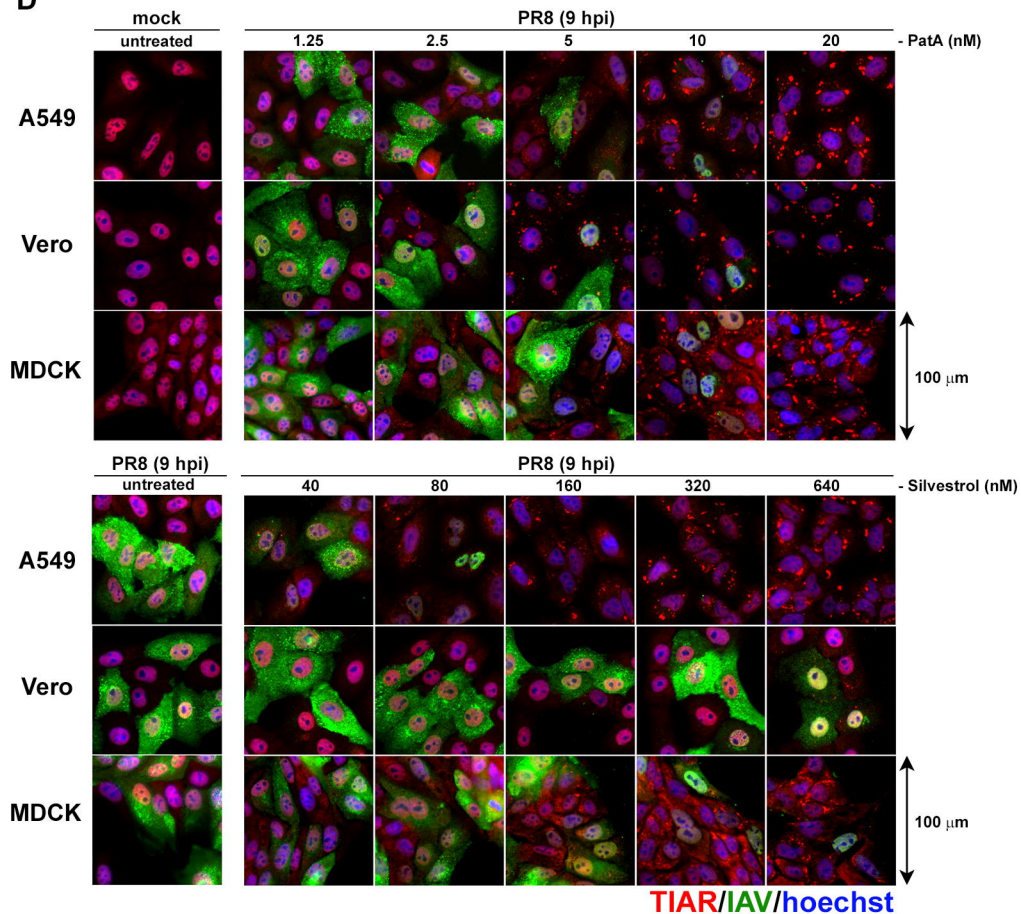
528

529 **Figure 5. Silvestrol and pateamine A block replication of H3N2 strain of IAV.** (A-C) A549 cells were

530 infected with A/Udorn/72(H3N2) strain of IAV and treated with 320 nM silvestrol at 4 hpi. Total RNA
531 and whole cell protein lysates were collected at 4, 8, and 12 hpi. The accumulation of viral NS segment
532 vRNA (A) and NS1 mRNA (B) was measured using RT-qPCR, and the accumulation of viral proteins
533 was analysed by western blotting (C). (D) Production of infectious virus progeny (Udorn strain) at 24 hpi
534 was measured using plaque assay. A549 cells were infected with MOI = 0.1 and treated with the
535 increasing concentrations of pateamine A at 1 hpi. Error bars represent standard deviations (n = 2).

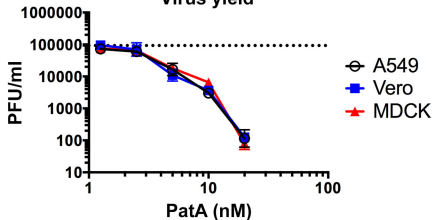


D

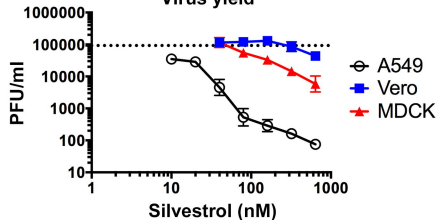


A

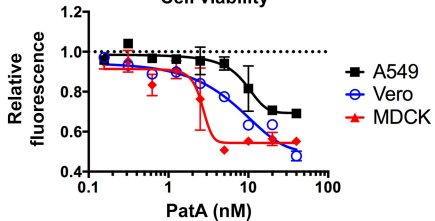
Virus yield

**B**

Virus yield

**C**

Cell viability

**D**

Cell viability

